[CANCER RESEARCH 64, 3296–3301, May 1, 2004]

Expression, Up-Regulation, and Transport Activity of the Multidrug-Resistance Protein Abcg2 at the Mouse Blood-Brain Barrier

Salvatore Cisternino, Claire Mercier, Fanchon Bourasset, Françoise Roux, and Jean-Michel Scherrmann

Institut National de la Santé et de la Recherche Médicale U26, Hôpital Fernand Widal, Paris, France

ABSTRACT

The breast cancer resistance protein (BCRP/ABCG2) is, like P-glycoprotein (P-gp), a member of the ABC family of drug transporters. These proteins actively transport various anticancer drugs from cells, causing multidrug resistance. The physiological expression of P-gp/ABCB1 at the blood-brain barrier (BBB) effectively restricts the brain uptake of many antitumor drugs by mediating their active efflux from the brain to the blood vessel lumen. However, little is known about the function of Abcg2 at the BBB *in vivo*. We used *in situ* brain perfusion to measure the uptake of two known Abcg2 substrates, prazosin and mitoxantrone, and the nonsubstrate vinblastine by the brains of wild-type and P-gp-deficient mutant *mdr1a*(−/−) mice with or without the P-gp/Abcg2 inhibitor GF120918 or the P-gp inhibitor PSC833. P-gp had no effect on the brain transport of prazosin and mitoxantrone at the mouse BBB, but wild-type and P-gp-deficient mouse brains perfused with GF120918 or a high concentration of prazosin showed carrier-mediated effluxes of prazosin and mitoxantrone from the brain that did not involve P-gp. In contrast, the brain uptake of vinblastine was restricted only by P-gp and not by Abcg2 at the BBB. The amounts of *abcg2* mRNA in cortex homogenates and capillary-enriched fractions of wild-type and *mdr1a*(−/−) mouse brains were measured by real-time quantitative reverse transcription-PCR. There was ~700-times more *abcg2* mRNA in brain microvessels than in the cortex of the wild-type mice, confirming that Abcg2 plays an important role at the BBB. There was also ~3 times more *abcg2* mRNA in the microvessels from P-gp-deficient mutant mouse brains than in the microvessels of wild-type mouse brains. These findings confirm that Abcg2 is a physiological transporter at the BBB that restricts the permeability of the brain to its substrates *in vivo*. Lastly, the defective P-gp in the mutant *mdr1a*(−/−) mice was associated with increased *abcg2* mRNA at the BBB and a greater export of prazosin and mitoxantrone from the brain, as measured in the P-gp-deficient mice *versus* the wild-type mice.

INTRODUCTION

Much of the specificity of the endothelium forming the blood-brain barrier (BBB) is due to the tight junctions between adjacent brain endothelial cells. These restrict the entry of compounds by paracellular diffusion from the blood to the brain and *vice versa*. The transcellular diffusion of compounds through the membrane bilayer of the brain endothelial cells may also be limited by transmembrane efflux transporters that belong to the ABC superfamily, such as P-glycoprotein (P-gp). P-gp was first described as a component of the acquired multidrug resistance (MDR) mechanism of tumor cells, but it is now known to be present physiologically at the luminal membrane of the brain capillary endothelial cells (1). P-gp/mdr1a actively expels a wide spectrum of amphiphilic drugs from the brain into the blood, leading to a decrease in their uptake by the brain (1). Another member of the ABC superfamily, which was first called BCRP or MXR and is now designated ABCG2 in the HUGO[1] nomenclature, confers resistance to many drugs, including mitoxantrone (MX), prazosin (PRA), the anthracyclines, and some camptothecin derivatives, and its range may overlap with the substrates of other P-gp and/or MDR-associated proteins (MRPs; Refs. 2–6). ABCG2 was recently identified in human and porcine brain capillary endothelial cells (7–10) and found to be responsible for the *in vitro* export of daunorubicin from porcine brain capillary endothelial cells (9). *In vivo* studies on Abcg2-deficient knockout mice have shown that Abcg2 is involved in the handling of and protection from porphyrins, such as chlorophyll and heme. Its ability to limit the oral availability of topotecan also suggests that it plays a role in intestinal absorption (11).

Whereas the action of ABCG2 in making cells drug resistant has been explored to some extent, knowledge of how ABCG2 mediates drug transport at the BBB *in vivo* could provide important information on the overall mechanisms underlying drug transfer, drug delivery and CNS toxicity. Recent *in vitro* studies showing that ABCG2 is present in brain endothelial cells raise the question of how it influences the efflux of drugs at the BBB *in vivo* (7–10).

The *in situ* brain perfusion method developed in the rat (12) and more recently in mice (13–15) is a very sensitive method for assessing drug transport at the luminal membrane of the endothelial cells of the BBB *in vivo*. It can be used to measure both the rate and mechanisms of transport. This technique respects the physiological properties of transport by maintaining the physiological properties of the BBB (13, 16). One of its great advantages is that there is no systemic exposure before its transport through the BBB, thus allowing the drug concentration in the perfusion fluid to be controlled and avoiding confounding factor of systemic disposition such as the effect of metabolism. We used the *in situ* brain perfusion technique in wild-type (wt) and P-gp-deficient mutant *mdr1a*(−/−) mice to check and exclude P-gp mechanisms from the interpretation of the data. The presence of Abcg2-mediated transport at the mouse BBB was assessed *in vivo* by measuring the brain transport of MX and PRA, which interact with P-gp and Abcg2 *in vitro*. Unlike PSC833, which inhibits P-gp transport, GF120918 inhibits both P-gp- and Abcg2-mediated transport (17, 18). The transport of MX, PRA, and vinblastine (VBL), which is not transported by ABCG2 (19), were then measured in wt and *mdr1a*(−/−) mice with and without GF120918 or PSC833. These multiple experimental strategies enabled us to show that the uptake of MX and PRA by the brain is not significantly affected by P-gp, unlike that of VBL. Real-time quantitative reverse transcription-PCR (RT-PCR) of brain parietal cortex homogenates and a capillary-enriched fraction isolated by the capillary depletion method confirmed that there is more *abcg2* mRNA in brain capillaries than in the cortex. We also show that the concentration of *abcg2* mRNA in the brain capillaries of mice lacking *mdr1a* is above normal. This increased *abcg2* mRNA in *mdr1a*(−/−) mutant mice was correlated with a greater *in vivo* brain efflux transport of PRA and MX in P-gp-deficient mice than in wt mice. These results therefore indicate that Abcg2 is normally present and functional at the luminal membrane of the brain endothelial cells of both wt and mutant *mdr1a*(−/−) mice, where it limits the uptake of its substrates by the brain.

Received 7/8/03; revised 1/23/04; accepted 2/26/04.

Grant support: INSERM.

The costs of publication of this article were defrayed in part by the payment of page charges. This article must therefore be hereby marked *advertisement* in accordance with 18 U.S.C. Section 1734 solely to indicate this fact.

Requests for reprints: Salvatore Cisternino, INSERM U26, Hôpital F. Widal, 200, rue du Fbg Saint-Denis, 75475 Paris cedex 10, France. Phone: 33-1-40054343; Fax: 33-1-40344064; E-mail: Salvatore.Cisternino@fwidal.inserm.fr.

[1] http://www.gene.ucl.ac.uk/nomenclature/.

MATERIALS AND METHODS

Animals

Adult male CF-1 mice [wt and mutant *mdr1a*(−/−); 30–40 g, 7–9 weeks of age] were bred in house from progenitors, initially obtained from Charles River Laboratories (Wilmington, MA), genotyped for mdr1a P-gp. The mice were housed in a controlled environment (22 ± 3°C with 55 ± 10% relative humidity) and maintained under a 12-h dark:light cycle (light from 6:00 a.m. to 6 p.m.). They had access to food and tap water *ad libitum*. All experimental procedures complied with the ethics rules of the French Ministry of Agriculture for experimentation with laboratory animals (law no. 87-848).

In Situ Brain Perfusion

Surgery and Perfusion. The transport of [^{3}H]MX (Moravek, Brea, CA), [^{3}H]PRA and [^{3}H]VBL (Amersham Pharmacia Biotech, Orsay, France) into the brain was measured by *in situ* brain perfusion (13). Briefly, mice were anesthetized by i.p. injection of ketamine-xylazine (140 and 8 mg/kg, respectively). The right external carotid was ligated rostral to the occipital artery at the level of the bifurcation of the common carotid. The caudal side of the right common carotid was ligated, and the cranial side was catheterized (polyethylene tubing; 0.30 mm inner diameter × 0.70 mm outer diameter; Biotrol Diagnostic, Chenevières-les-Louvres, France). The syringe containing the perfusion liquid was placed in an infusion pump (Harvard PHD 2000; Harvard Apparatus, Holliston, MA) and connected to the catheter. The thorax was opened, and the heart was cut before starting the perfusion. Perfusion was at a flow rate of 2.5 ml/min. The perfusion fluid consisted of bicarbonate-buffered physiological saline containing 128 mM NaCl, 24 mM $NaHCO_3$, 4.2 mM KCl, 2.4 mM NaH_2PO_4, 1.5 mM $CaCl_2$, 0.9 mM $MgCl_2$, and 9 mM D-glucose. The solution was gassed with 95% O_2–5% CO_2 for pH control (7.4) and warmed to 37°C in a water bath. Each mouse was perfused with tritiated tracer and [^{14}C]sucrose (0.2 μCi/ml; Perkin-Elmer, Paris, France) added to the perfusion fluid. Brain perfusion was terminated by decapitating the mouse at a selected time (30, 60, 90, or 120 s). The brain was removed from the skull and dissected out on ice. The right cerebral hemisphere and aliquots of the perfusion fluid were placed in tared vials and weighed. Samples were digested in 2 ml of Solvable (Packard, Rungis, France) at 50°C and mixed with 9 ml of Ultima Gold XR (Packard). Dual label counting was performed in a Packard Tri-Carb 1900TR.

Calculation of Apparent Brain Distributional Volume and Initial Brain Uptake. All of the calculations have been described previously (13–16). The brain vascular volume of each animal was assessed with the vascular marker [^{14}C]sucrose. This, like inulin, does not measurably cross the BBB during short perfusions (12). In the perfusion experiments, [^{14}C]sucrose was perfused together with the tritium-labeled substrates to estimate the brain vascular volume (V_{vasc}; μl/g) as:

$$V_{vasc} = X^*/C^*_{perf} \quad (A)$$

where X^* (dpm/g) is the amount of sucrose in the right brain hemisphere and C^*_{perf} (dpm/μl) is the concentration of [^{14}C]sucrose in the perfusion fluid.

The apparent brain distribution volume was calculated from the amount of radioactivity in the right brain hemisphere by the formula:

$$V_{brain} = X_{brain}/C_{perf} \quad (B)$$

where X_{brain} (dpm/g) is the calculated amount of tritium-labeled compound in the right cerebral parenchyma, and C_{perf} (dpm/μl) is the concentration of tritium-labeled tracer in the perfusion fluid. Brain tissue total radioactivity was corrected for vascular contamination with the following formula:

$$X_{brain} = X_{tot} - V_{vasc}C_{perf} \quad (C)$$

where X_{tot} (dpm/g) represents the total quantity of tritium-labeled tracer trapped within the brain parenchyma and cerebrovasculature capillary bed. Subtraction of the intravascularly located tritium-labeled compound from the total amount of tritium-labeled compound yielded the amount in the brain parenchyma.

Initial brain transport was expressed as a K_{in} (μl/s/g) and was calculated from the formula:

$$K_{in} = V_{brain}/T \quad (D)$$

where T is the perfusion time (s).

Trans Influx Zero Transport Studies. A time-course study of the apparent distributional brain volume of the tritiated drugs (0.3–0.4 μCi/ml) was done in wt mice to select an appropriate brain perfusion time. The initial uptake of tritiated drugs into the mouse brain after 120 s of perfusion was measured in wt and *mdr1a*(−/−) mice with and without inhibitors. Inhibitors were added to the perfusion fluid to control exposure at the BBB and to avoid systemic metabolic processes. The inhibitors were PSC833 (3 μM; kindly provided by Novartis, Basel, Switzerland) and GF120918 (2 μM; kindly provided by Glaxo SmithKline, Les Ulis, France). The uptake of labeled MX, PRA, and VBL was also measured in the presence of unlabeled MX (100 μM; Sigma, St Quentin, France), PRA (30 μM; Sigma), or VBL (150 μM; Lilly, Saint Cloud, France), respectively. The stock solutions of PRA, GF120918, and PSC833 were prepared in DMSO. MX and VBL were dissolved in 0.9% NaCl. All solutions were prepared fresh on the day of the experiment and diluted with the bicarbonate-buffered saline used for perfusion. The final DMSO concentration in the perfusion fluid was always 0.5% (v/v); this concentration did not alter the integrity of the BBB, as measured by the permeability of [^{14}C]sucrose.

Capillary Depletion

The blood was removed from the brains of the mice before microvessels were extracted to minimize contamination with blood cells and hemoglobin in the quantitative RT-PCR study. The mice were perfused with saline by *in situ* brain perfusion for 30 s. They were then decapitated, and the brain was removed and cleaned of meninges on ice. The capillary depletion method of Triguero *et al.* (20) was used with some modifications (21) to obtain capillary-enriched fractions of wt and *mdr1a*(−/−) mouse brains. The blood-free brains of six wt or *mdr1a*(−/−) mice were pooled and homogenized with a glass homogenizer (15 pestle strokes) in 3.5 ml of buffer [10 mM HEPES, 141 mM NaCl, 4 mM KCl, 1 mM NaH_2PO_4, 2.8 mM $CaCl_2$, 1 mM $MgSO_4$ and 10 mM D-glucose (pH 7.4)] at 4°C. Chilled 37% dextran solution was then added to obtain a final dextran concentration of 18.5%. All homogenizations were performed rapidly at 4°C. The homogenates were centrifuged at 5400 × *g* for 15 min at 4°C in a swinging-bucket rotor, and the supernatants were carefully removed. Brain capillaries are separated from the parenchymal elements by a well-developed collagenous basal membrane as in the vasculature of peripheral organs, but the neural and glial elements of the brain lack significant amounts of nonvascular collagenous matrix, whereas most peripheral organs have abundant mesenchymal collagen networks. Thus, physical fractionation of this soft tissue efficiently separates central nervous system microvessels from the brain parenchyma (22, 23). The homogenates were centrifuged through a dextran gradient, and the pellet (composed of blood-free intact microvessels segments and brain nuclei) was collected (20). Mechanical homogenization of brain tissue rapidly provided brain capillaries, minimizing mRNA denaturation due to RNase activity and changes in cell phenotype, unlike time-consuming enzymatic methods (23). Microvessel purity was checked by measuring γ-glutamyl transpeptidase activity because this enzyme is abundant in the endothelial cells of the BBB (22). The enzyme activities in aliquots of the supernatant and pellet confirmed that there was ~30 times more activity in the pellet than in the supernatant. The pellet was removed and placed in RNAlater (Qiagen, Courtaboeuf, France) at −20°C until RNA extraction.

Total RNA Extraction and Real-Time Quantitative RT-PCR

Total RNA was extracted from isolated mouse brain capillaries and parietal cortex by use of the RNeasy Mini (Qiagen) extraction kit according to the manufacturer's instructions. The RNA concentration and integrity of each sample were evaluated with the RNA 6000 LabChip kit (Agilent Biotechnologies, Massy, France) with the Agilent 2100 Bioanalyzer. The RNA samples (5 μg) were made up to 31 μl with PCR water, heated at 65°C for 10 min, and cooled on ice (4 min) before reverse transcription. We then added 2 μl of Oligo(dT) (Roche Diagnostic, Meylan, France) to each tube to obtain a final volume of 33 μl [with 10 mM Oligo(dT)], and this volume was transferred to a tube of First-Strand Reaction Mix Beads (Amersham Pharmacia Biotech). The tubes were placed on ice, homogenized by gentle vortexing for 10 min, and then incubated at 37°C for 60 min.

The sequences of the primers for the target gene *abcg2* (accession no.

AF140218) were obtained with Primer Express software (Applied Biosystems, Courtaboeuf, France) to minimize the formation of internal structures. The primers themselves were synthesized by Genset (Paris, France).

The forward primer was 5′-AGCTCCGATGGATTGCCAG-3′ (nucleotides 1146–1164), and the reverse primer was 5′-GAGGGTTCCCGAGCAAGT-TT-3′ (nucleotides 1196–1177). The annealing temperature was 81°C, and the amplicon size, evaluated with the DNA 500 Bio Sizing kit (Agilent Biotechnologies) and Agilent 2100 Bioanalyzer, was 51 bp. TaqMan Rodent *gapdh* Control Reagents (Applied Biosystems) were used as normalization controls. The products of RT-PCR were diluted to have the same cDNA concentration (10 ng/μl) in all samples. One μl of each RT-PCR dilution, 1 μl of water (no template control), or 1 μl of 10 ng/μl RNA pool (no amplification control) was added to 49 μl of mixture containing 25 μl of SYBR Green PCR Master Mix (Applied Biosystems), 300 nM sense and antisense primer, and PCR water for *abcg2* and 25 μl of TaqMan PCR Master Mix (Applied Biosystems), 0.5 μl of primer 1, 0.5 μl of primer 2, 0.5 μl of probe, and PCR water. Samples were placed in a thermal cycler and cycled 40 times (denaturation at 95°C for 15 s and 60°C for 60 s, and polymerization at 81°C for 60 s).

Increasing amounts of standard cDNA were used with gene-specific primers and fluorescent probes to generate a standard curve displaying a linear relationship between the threshold cycle (C_T; number of cycles at which the fluorescence signal reaches a defined threshold) and the logarithm of the initial template concentration. The equation describing the standard curve for *abcg2* was $Y = -2.05X + 30.4$ and that for *gapdh* was $Y = -2.2X + 28.8$. The efficiencies for *abcg2* and *gapdh* were approximately equal. The absolute value of the slope of log input *versus* ΔC_T (C_T *abcg2* − C_T *gapdh*) was 0.023 (<0.1 theoretical).

Dissociation curve analysis was performed after amplification to confirm that the expected product was generated and to distinguish specific from nonspecific products and primer-dimers. The thermal protocol for the dissociation was 15 s at 95°C, followed by 20 s at 60°C and a slow ramp (1.75°C/min) over 20 min from 60°C to 95°C. The data for the dissociation curve were captured during the slow ramp. We also analyzed the PCR product by agarose gel electrophoresis with the DNA Bio Sizing kit to determine the quality of the PCR.

Statistical Analysis

The K_{in} values are the means ± SD of four to six mice unless specified otherwise. Student's unpaired *t* test was used to identify significant differences between groups when appropriate. The tests were all two-tailed, and statistical significance was set at $P < 0.05$. Three experiments were performed for RT-PCR, and the data are means of the *abcg2* mRNA concentration divided by the *gapdh* mRNA concentration ± SD. Data were analyzed by two-way ANOVA followed by Dunnett's test, and statistical significance was set at $P < 0.01$ or $P < 0.001$.

RESULTS

Assessment of BBB Integrity. The mouse brain vascular volume (16 ± 2 μl/g) agreed with normal distribution volume for sucrose (12–14); in all brain transport experiments. A brain vascular volume that exceeded 20 μl/g was considered to reflect a loss of BBB physical integrity; in those cases brain transport parameters were not calculated (13, 16). Brain perfusions performed with MX concentrations >100 μM were associated with a loss of BBB integrity, preventing measurement of the [^{3}H]MX brain transport at the highest MX concentrations.

Time Course of Brain Uptake. The uptake of MX, PRA, and VBL by the brains of wt mice, expressed as apparent brain distributional volume (V_{brain}), was measured at different brain perfusion times to select an appropriate perfusion time (Fig. 1). The perfusion time selected for single-time brain uptake studies ensured that at least 40% of the total radioactivity of the tritiated drug in the tissue resided outside the vascular space (12). Given a vascular volume of 14–18 μl/g, a drug brain volume V_{brain} at 9–12 μl/g is equivalent to 40% of the radioactivity in the extravascular space. This requirement was strictly met at 30 s for MX and PRA and at 60 s for VBL (Fig. 1). Therefore, a perfusion time of 120 s was used for all of the single-time uptake studies because it provided optimum sensitivity for transport measurements in various experimental situations, whereas uptake remained linear (16).

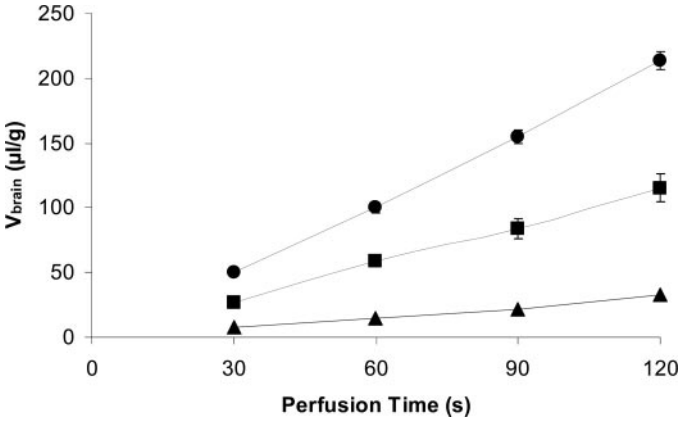

Fig. 1. Time course of [^{3}H]vinblastine (▲), [^{3}H]prazosin (■), and [^{3}H]mitoxantrone (●) uptake by the right brain hemispheres of wild-type mice, expressed as apparent brain distribution volume (V_{brain}, μl/g) determined by *in situ* brain perfusion. Data are means ± SD (*bars*) of four to five animals per data point.

Influence of mdr1a P-gp on the Brain Transport of MX, PRA, and VBL without Recourse to Inhibitors in wt and *mdr1a*(−/−) Mice. Because many of the drugs transported by Abcg2 are, like MX and PRA, also carried by other transporters, such as P-gp, the effect of P-gp on the transport of the three selected drugs was also measured in the two mouse strains. Animals lacking specific transporters are ideal and efficient tools for evaluating the contribution of transporters such as P-gp to the transport of drugs in the brain without the need for inhibitors (14). We measured the brain transport of the three selected substrates in wt and P-gp-deficient mice to assess the influence of P-gp on their brain uptake. The uptake of VBL was ~2-fold greater in mice lacking P-gp than in wt mice, confirming that P-gp limits initial VBL uptake at the mouse BBB (Fig. 2*A*). The transport of PRA was not affected by P-gp (Fig. 2*B*), as shown by the data for *mdr1a*(−/−) (1.14 ± 0.06 μl/s/g) and wt (0.96 ± 0.09 μl/s/g) mice. The brains of *mdr1a*(−/−) mice took up significantly lesser MX (1.55 ± 0.05 μl/s/g; $P < 0.01$) than did those of wt mice (1.78 ± 0.06 μl/s/g; Fig. 2*C*). This result gave no clear information about the influence of P-gp on the brain transport of MX. It probably indicates that a non-P-gp efflux, perhaps Abcg2 transport (see below), is enhanced in the *mdr1a*(−/−) mice.

Effect of Inhibition of P-gp by PSC833 on the Brain Transport of MX, PRA, and VBL in wt and *mdr1a*(−/−) Mice. Chemical modulation could be a way to determine the existence of a carrier-mediated transport, despite the lack of specificity. PSC833, a cyclosporin analog, inhibits P-gp efflux but not Abcg2 transport *in vitro* (2). We therefore could use PSC833 to measure the P-gp transport component in wt mice and help to confirm our results obtained with *mdr1a*(−/−) mice. PSC833 increased the brain uptake of VBL in wt mice to be significantly greater than in wt mice not given PSC833 (Fig. 2*A*), but the brain uptake of VBL in wt mice given PSC833 was not different from that in P-gp-deficient mice (Fig. 2*A*). The uptake of PRA and MX by the brains of wt mice was not significantly different with or without PSC833 (Fig. 2, *B* and *C*). Thus, P-gp does not significantly limit the brain uptake of PRA or MX at the mouse BBB.

Effect of GF120918 on MX, PRA, and VBL Transport in Brains of wt and *mdr1a*(−/−) Mice. GF120918, an effective inhibitor of P-gp and Abcg2 transport, was perfused with MX, PRA, and VBL in

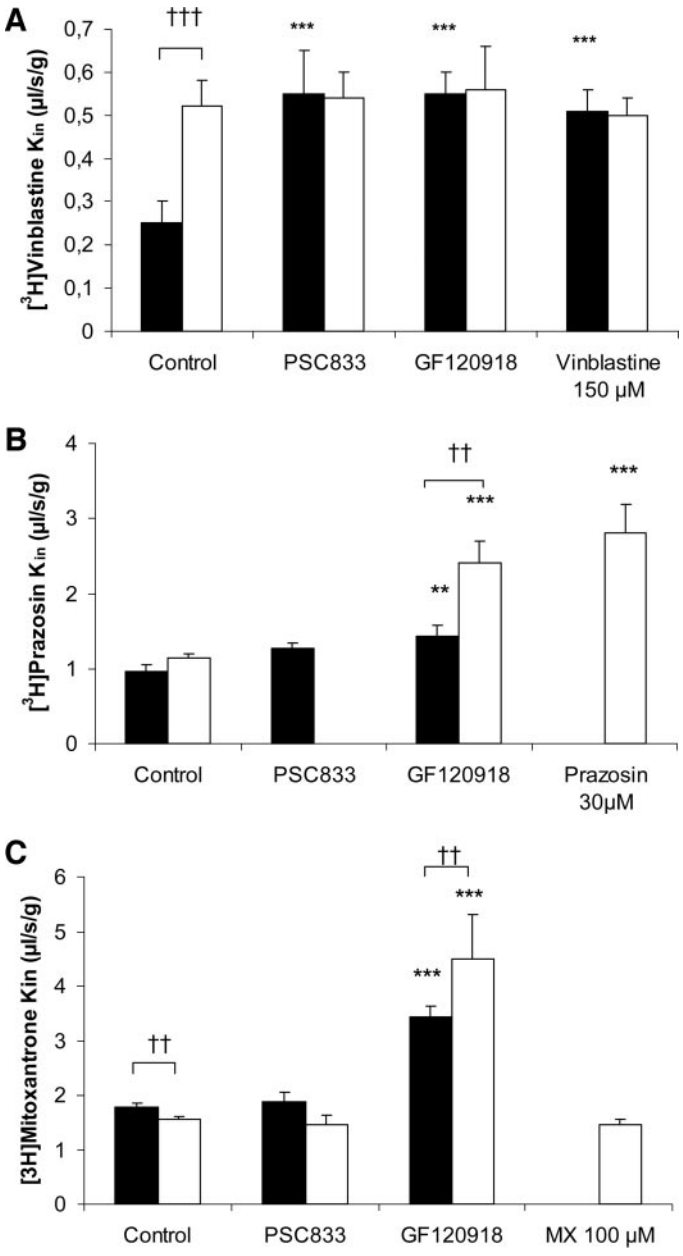

Fig. 2. Brain transport coefficients (K_{in}, µl/s/g) for [^{3}H]vinblastine (*A*), [^{3}H]prazosin (*B*), and [^{3}H]mitoxantrone (*MX*; *C*) in wild-type (■) and *mdr1a*(−/−) mice (□) measured by *in situ* brain perfusion with or without coperfusion of GF120918 (2 µM), PSC833 (3 µM), prazosin (30 µM), or mitoxantrone (100 µM). The mice were perfused via the common carotid artery for 120 s. Data are means ± SD (*bars*) of four animals. **, $P < 0.01$; ***, $P < 0.001$ for control *versus* PSC833, GF120918, mitoxantrone, or prazosin coperfused mice in each strain. ††, $P < 0.01$; †††, $P < 0.001$ for wild-type *versus* *mdr1a*(−/−) mice coperfused with the same compound.

wt and *mdr1a*(−/−) mice to determine the influence of Abcg2 on their brain transport. Because of the lack of P-gp transport of MX and PRA at the mouse BBB, GF120918 inhibited only Abcg2-mediated transport of these two substrates in wt mice. In contrast to MX and PRA, VBL was significantly transported by P-gp at the mouse BBB. The uptake of VBL by the brains of wt mice was significantly increased by GF120918 over that of wt mice not receiving GF120918 (Fig. 2*A*). Moreover, the uptake of VBL by the brains of *mdr1a*(−/−) mice was not affected to any great extent by GF120918. The uptake of VBL at the mouse BBB is thus restricted by P-gp and not by Abcg2. The brain transport of PRA in wt mice was increased 1.5-fold by perfusion together with GF120918, and that of MX was increased 2-fold, compared with control wt mice not receiving inhibitor (Fig. 2, *B* and *C*). The brain transport of PRA was increased 2.1-fold and that of MX 3.0-fold in *mdr1a*(−/−) mice when the drugs were perfused together with GF120918 compared with P-gp-deficient mice not receiving perfusions containing this inhibitor. GF120918 had a statistically greater effect on the brain transport of PRA (0.67-fold) and MX (0.71-fold) in *mdr1a*(−/−) mice than on their transport in wt mice (Fig. 2, *B* and *C*).

Saturation of Carrier-Mediated Transport. The brains of P-gp-deficient and/or wt mice were perfused with labeled PRA, MX, or VBL plus high concentrations of the unlabeled drug to determine whether efflux could be saturated at the mouse BBB. PRA and VBL efficiently inhibited their own efflux at the BBB, but unlabeled VBL increased the uptake of [^{3}H]VBL (Fig. 2*A*) by completely saturating P-gp transport. PRA also inhibited its own efflux in P-gp-deficient mice with the same efficiency as GF120918 in P-gp-deficient mice (Fig. 2*B*). MX (100 µM) did not inhibit its own brain transport, probably because of a lower affinity and despite the fact that its transport at the mouse BBB is carrier-mediated.

Real-Time Quantitative RT-PCR in Cortex Homogenates and Capillary-Enriched-Fractions from wt and *mdr1a*(−/−) Mice. The *abcg2* mRNA values were normalized with reference to the *gapdh* mRNA in each sample. The dissociation curves show the products from a one-step RT-PCR for a *abcg2* target as well as for a no-template control (water), indicating the specificity of the PCR. The amplicon from the main product was detected with a melting temperature of 77°C. We also analyzed a PCR product of the capillary-enriched wt brain fraction by agarose gel electrophoresis to determine the quality of the PCR (Fig. 3*A*). Only two PCR products were observed in the lane, and their molecular sizes were 51 bp for *abcg2* and 177 bp for *gapdh*, as expected (Fig. 3*A*). The brain capillaries of wt mice had significantly more (~700 times) *abcg2* mRNA (675 ± 50; $n = 3$) than the brain cortex (1 ± 0.2; $n = 3$; $P < 0.001$). There was 3 times more ($P < 0.01$) *abcg2* mRNA in the brain capillaries of *mdr1a*(−/−) mice (2254 ± 181; $n = 3$) than in wt capillaries (Fig. 3*B*).

DISCUSSION

In this study, we found that the transport of VBL in the brain is mediated by P-gp, whereas the transport of MX and PRA across the BBB depends mainly on the presence of Abcg2 at the luminal membrane of the mouse brain microvessels. PRA, like progesterone, interacts with P-gp via the P-gp regulatory/allosteric site, which does not allow any apparent transport of drugs (24–26). Overproduction of P-gp usually results in only modest resistance to MX (27, 28), implying that this drug is poorly transported by P-gp (28). The ABC transporter Mrp1 has a moderate and controversial effect in conferring resistance to MX, as shown in mouse cells lacking ABC transporters (28, 29) and cells transfected with *MRP1* (30). Nevertheless, we recently showed that Mrp1 is not functional at the luminal side of the mouse BBB (15). The present study demonstrates that Abcg2 is a major factor controlling MX and PRA transport at the BBB of wt mice.

Vinca alkaloid drugs, such as VBL, are not transported by Abcg2, whereas MX and PRA are efficiently transported *in vitro* (6, 17, 19). We investigated Abcg2-mediated transport at the BBB by measuring the transport of MX, PRA, and VBL with and without GF120918, which inhibits P-gp and Abcg2 transport, and PSC833, which inhibits P-gp. The results indicate that VBL transport at the mouse BBB is not restricted by Abcg2. In contrast, the brain transport of PRA and MX is not sensitive to PSC833 but is significantly increased by GF120918 in wt mice. Thus, a mechanism unrelated to P-gp mediates the brain

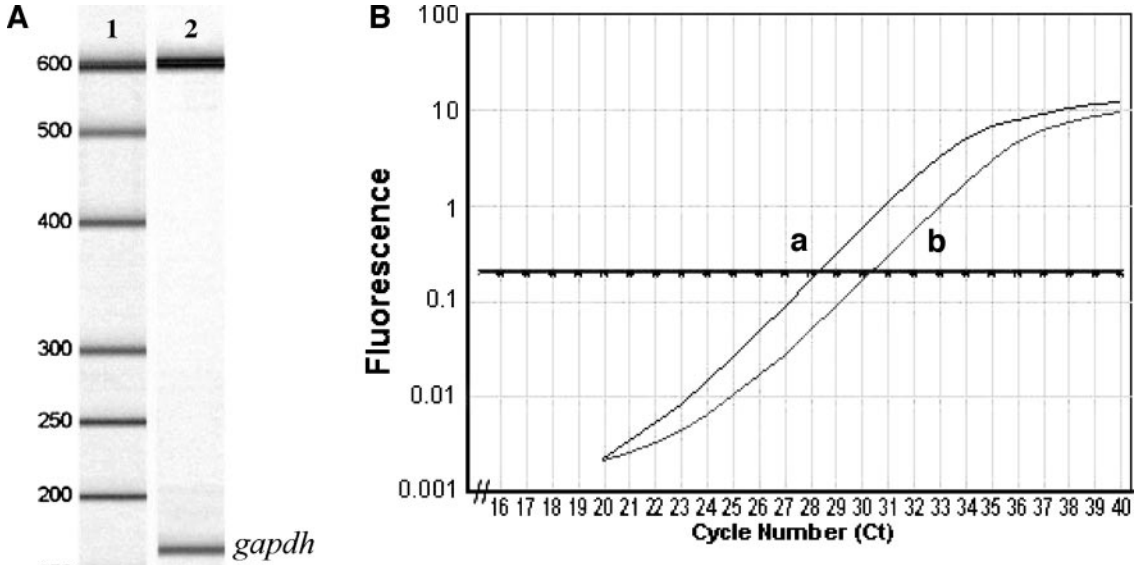

Fig. 3. PCR product analysis. *A*, products from capillary-enriched wild-type brain fractions were separated by agarose gel electrophoresis using the DNA Bio Sizing kit. The molecular ladder is shown in *Lane 1* and PCR products in *Lane 2*. There were only two PCR products in *Lane 2*, except for the two size calibrators. The PCR products were 51-bp long for *abcg2* and 177-bp long for *gapdh*, as expected. *B*, example of one amplification curve obtained for the *abcg2* cDNA of the wild-type mice (*b*) and the *mdr1a*(−/−) (*a*) brain capillaries by real-time PCR. There was 3 times more *abcg2* cDNA in *mdr1a*(−/−) brain capillaries than in wild-type mice brain capillaries after normalization with the *gapdh* threshold cycle (*Ct*).

efflux of MX and PRA at the BBB. Although P-gp does not limit MX or PRA uptake at the BBB of wt mice, we perfused the brains of mutant mice lacking P-gp to clearly reveal this non-P-gp transport. The brain uptake of PRA was increased 2.1-fold and that of MX 3.0-fold in *mdr1a*(−/−) mice when the drugs were perfused together with GF120918 compared with their uptake by P-gp-deficient mice not perfused with this inhibitor. PSC833 also had no effect on the brain transport of MX or PRA at the BBB in P-gp-deficient mice, confirming *in vivo* that it does not overcome Abcg2 resistance. The inhibition of the brain transport of PRA and MX by GF120918 confirms the existence of a mechanism unrelated to P-gp, probably Abcg2-mediated transport, at the mouse BBB. We also inhibited the carrier-mediated transport of PRA and MX by use of a high concentration of unlabeled compound. PRA (30 μM) inhibited the efflux of radiolabeled PRA in *mdr1a*(−/−) mice, whereas 100 μM MX did not inhibit its own efflux. Higher concentrations of MX were not perfused because of their adverse effect on the BBB.

Surprisingly, GF120918 had a greater effect on the brain transport of PRA (0.67-fold) and MX (0.71-fold) in *mdr1a*(−/−) mice than on their transport in wt mice. The brain transport of MX was also lower in mice lacking P-gp than in the wt mice. We therefore postulate that Abcg2 is up-regulated in P-gp-deficient mice or that the mediated-drug efflux is more rapid in this *mdr1a*-deficient mouse strain. The first possibility was checked by measuring *abcg2* mRNAs in the brain cortex and capillaries by quantitative real time RT-PCR. The brain capillaries of wt mice had significantly (~700 times) more *abcg2* mRNA than the brain cortex. A recent report also showed significantly more *abcg2* mRNA in the capillary endothelial cells of pig brains than in the whole brain (9). This again points to the importance of Abcg2 in brain capillaries, as suggested by the MX and PRA *in situ* brain transport studies, given that Abcg2 tends to be concentrated in brain microvessel cells. One concern about the use of capillary microvessels could be the cell extract composition. Isolated brain capillaries contain approximately one-third pericytes and some astrocyte endfoot membranes (23). The endothelial cells, like pericytes, could contain the *abcg2* mRNA measured in our experiments. However, pericytes from pig brains contain no *abcg2* mRNA as measured by Northern blotting (9). Moreover, *in situ* brain perfusion measures only the transport at the luminal membrane of endothelial brain cells (16). These observations together suggest that Abcg2 is located at the luminal membrane of the brain microvessels. We also found that the brain capillaries of *mdr1a*(−/−) mice contain 3 times more *abcg2* mRNA than wt capillaries. These data confirm our transport studies indicating that Abcg2 synthesis is increased in *mdr1a*(−/−) mouse brain capillaries. This *abcg2* increase is probably correlated with the overproduction of the Abcg2 protein at the mouse BBB. The Abcg2 protein level is well correlated with resistance to MX and PRA *in vitro* (31). Although Abcg2 overproduction by drug selection in human or murine cells could be associated with a mutation at residue 482 that affects the specificity and transport function of the pump (6, 32), such alterations remain to be established *in vivo* for the increased Abcg2 in *mdr1a*(−/−) mice. However, the inhibitor GF120918 also reverses wt protein and Abcg2 with the 482 polymorphism (6). We have yet to determine whether a lack of mdr1a directly results in compensation involving Abcg2. The basal amount of Mrp1 is slightly elevated in cells from knockout mouse embryos lacking functional mdr1a/1b, but the basal amounts of Abcg2 in wt cells and cells lacking P-gp remain to be determined (28). There is a lack of functional mdr1a in two

situations *in vivo*. One is in *mdr1a*(−/−) knockout mice that have increased *mdr1b* expression in the liver and the kidney but not in the brain or intestine, which normally contain little or no mdr1b (33). The other one is in CF-1 mutant mice lacking *mdr1a*(−/−), the mouse strain used in our study, where the amount of mdr1b is unaltered (34). Thus, the cause of the up-regulation remains to be clarified in mice lacking mdr1a, but it points to a tissue-specific compensation involving ABC transporters. Such compensation between drug transporters has yet to be explored in Abcg2(−/−) knockout mice. A recent study showed that there was more *ABCG2* in the brain capillaries extracted from a human glioblastoma than in nonmalignant brain tissue (10).

In conclusion, this study demonstrates that Abcg2 is physiologically present and functional at the mouse BBB. The basal expression is sufficient to limit the brain uptake of MX and PRA, so that Abcg2 is thus a newly identified factor limiting the permeability of the brain to drugs and a potential source of drug-drug interactions. We also found that the concentration and transport activity of Abcg2 *in vivo* are increased by a lack of mdr1a at the mouse BBB. This highlights the care that must be taken with deficient mouse models, in which compensatory gene expression and protein synthesis may offset the lack of a specific gene.

ACKNOWLEDGMENTS

We thank Dr. Owen Parkes for linguistic revisions.

REFERENCES

1. Sun H, Dai H, Shaik N, Elmquist WF. Drug efflux transporters in the CNS. Adv Drug Deliv Rev 2003;55:83–105.
2. Bates SE, Robey R, Miyake K, Rao K, Ross DD, Litman T. The role of half-transporters in multidrug resistance. J Bioenerg Biomembr 2001;33:503–11.
3. Litman T, Druley TE, Stein WD, Bates SE. From MDR to MXR: new understanding of multidrug resistance systems, their properties and clinical significance. Cell Mol Life Sci 2001;58:931–59.
4. Chen ZS, Robey RW, Belinsky MG, et al. Transport of methotrexate, methotrexate polyglutamates, and 17β-estradiol 17-(β-D-glucuronide) by ABCG2: effects of acquired mutations at R482 on methotrexate transport. Cancer Res 2003;63:4048–54.
5. Allen JD, Van Dort SC, Buitelaar M, van Tellingen O, Schinkel AH. Mouse breast cancer resistance protein (Bcrp1/Abcg2) mediates etoposide resistance and transport, but etoposide oral availability is limited primarily by P-glycoprotein. Cancer Res 2003;63:1339–44.
6. Allen JD, Jackson SC, Schinkel AH. A mutation hot spot in the Bcrp1 (Abcg2) multidrug transporter in mouse cell lines selected for Doxorubicin resistance. Cancer Res 2002;62:2294–9.
7. Cooray HC, Blackmore CG, Maskell L, Barrand MA. Localisation of breast cancer resistance protein in microvessel endothelium of human brain. Neuroreport 2002;13:2059–63.
8. Eisenblatter T, Galla HJ. A new multidrug resistance protein at the blood-brain barrier. Biochem Biophys Res Commun 2002;293:1273–8.
9. Eisenblatter T, Huwel S, Galla HJ. Characterisation of the brain multidrug resistance protein (BMDP/ABCG2/BCRP) expressed at the blood-brain barrier. Brain Res 2003;971:221–31.
10. Zhang W, Mojsilovic-Petrovic J, Andrade MF, Zhang H, Ball M, Stanimirovic DB. Expression and functional characterization of ABCG2 in brain endothelial cells and vessels. FASEB J 2003;17:2085–7.
11. Jonker JW, Buitelaar M, Wagenaar E, et al. The breast cancer resistance protein protects against a major chlorophyll-derived dietary phototoxin and protoporphyria. Proc Natl Acad Sci USA 2002;99:15649–54.
12. Takasato Y, Rapoport SI, Smith QR. An in situ brain perfusion technique to study cerebrovascular transport in the rat. Am J Physiol 1984;247:H484–93.
13. Dagenais C, Rousselle C, Pollack GM, Scherrmann JM. Development of an in situ mouse brain perfusion model and its application to mdr1a P-glycoprotein deficient mice. J Cereb Blood Flow Metab 2000;20:381–6.
14. Cisternino S, Rousselle C, Dagenais C, Scherrmann JM. Screening of multidrug-resistance sensitive drugs by in situ brain perfusion in P-glycoprotein-deficient mice. Pharm Res 2001;18:183–90.
15. Cisternino S, Rousselle C, Lorico A, Rappa G, Scherrmann JM. Apparent lack of Mrp1-mediated efflux at the luminal side of mouse BBB endothelial cells. Pharm Res 2003;20:904–9.
16. Smith QR. Brain perfusion systems for studies of drug uptake and metabolism in the central nervous system. In: Borchardt RT, Smith PL, Wilson G, editors. Models for assessing drug absorption and metabolism, Vol. 8. New York: Plenum Press, 1996. p. 285–307.
17. Allen JD, Brinkhuis RF, Wijnholds J, Schinkel AH. The mouse Bcrp1/Mxr/Abcp gene: amplification and overexpression in cell lines selected for resistance to topotecan, mitoxantrone, or doxorubicin. Cancer Res 1999;59:4237–41.
18. De Bruin M, Miyake K, Litman T, Robey R, Bates SE. Reversal of resistance by GF120918 in cell lines expressing the ABC half-transporter, MXR. Cancer Lett 1999;146:117–26.
19. Litman T, Brangi M, Hudson E, et al. The multidrug-resistant phenotype associated with overexpression of the new ABC half-transporter, MXR (ABCG2). J Cell Sci 2000;113:2011–21.
20. Triguero D, Buciak J, Pardridge WM. Comparison of in vitro and in vivo models of drug transcytosis through the blood-brain barrier. J Pharmacol Exp Ther 1990;253:884–91.
21. Rousselle C, Clair P, Lefauconnier JM, Kaczorek M, Scherrmann JM, Temsamani J. New advances in the transport of doxorubicin through the blood-brain barrier by a peptide vector-mediated strategy. Mol Pharmacol 2000;57:679–86.
22. Lattera J, Goldstein GW. Brain microvessels and microvscular cells in vitro. In: Pardridge WM, editor. The blood-brain barrier cellular and molecular biology. New York: Raven Press, 1993. p. 1–24.
23. Pardridge WM. Isolated brain capillaries: an in vitro model of blood-brain barrier research. In: Pardridge WM, editor. Introduction to the blood-brain barrier. Methodology, biology and pathology. Cambridge: Cambridge University Press, 1998. p. 49–62.
24. Shapiro AB, Fox K, Lam P, Ling V. Stimulation of P-glycoprotein-mediated drug transport by prazosin and progesterone. Evidence for a third drug-binding site. Eur J Biochem 1999;259:841–50.
25. Greenberger LM, Yang CP, Gindin E, Horwitz SB. Photoaffinity probes for the α1-adrenergic receptor and the calcium channel bind to a common domain in P-glycoprotein. J Biol Chem 1990;265:4394–401.
26. Martin C, Berridge G, Higgins CF, Mistry P, Charlton P, Callaghan R. Communication between multiple drug binding sites on P-glycoprotein. Mol Pharmacol 2000;58:624–32.
27. Dalton WS, Durie BG, Alberts DS, Gerlach JH, Cress AE. Drug-resistance in multiple myeloma and non-Hodgkin's lymphoma: detection of P-glycoprotein and potential circumvention by addition of verapamil to chemotherapy. J Clin Oncol 1989;7:415–24.
28. Allen JD, Brinkhuis RF, van Deemter L, Wijnholds J, Schinkel AH. Extensive contribution of the multidrug transporters P-glycoprotein and Mrp1 to basal drug resistance. Cancer Res 2000;60:5761–6.
29. Diah SK, Smitherman PK, Aldridge J, et al. Resistance to mitoxantrone in multidrug-resistant MCF7 breast cancer cells: evaluation of mitoxantrone transport and the role of multidrug resistance protein family proteins. Cancer Res 2001;61:5461–7.
30. Rajagopal A, Pant AC, Simon SM, Chen Y. In vivo analysis of human multidrug resistance protein 1 (MRP1) activity using transient expression of fluorescently tagged MRP1. Cancer Res 2002;62:391–6.
31. Robey RW, Honjo Y, van de Laar A, et al. A functional assay for detection of the mitoxantrone resistance protein, MXR (ABCG2). Biochim Biophys Acta 2001;1512:171–82.
32. Özvegy C, Varadi A, Sarkadi B. Characterization of drug transport, ATP hydrolysis, and nucleotide trapping by the human ABCG2 multidrug transporter. Modulation of substrate specificity by a point mutation J Biol Chem 2002;277:47980–90.
33. Schinkel AH, Smit JJM, Van Tellingen O, et al. Disruption of the mouse mdr1a P-glycoprotein gene leads to a deficiency in the blood-brain barrier and to increased sensitivity to drugs. Cell 1994;77:491–502.
34. Umbenhauer DR, Lankas GR, Pippert TR, et al. Identification of a P-glycoprotein-deficient subpopulation in the CF-1 mouse strain using a restriction fragment length polymorphism. Toxicol Appl Pharmacol 1997;146:88–94.